The Second Earth Trojan 2020 XL₅

Man-To Hui (許文韜)[1] , Paul A. Wiegert[2,3] , David J. Tholen[4] , and Dora Föhring[4]
[1] State Key Laboratory of Lunar and Planetary Science, Macau University of Science and Technology, Avenida Wai Long, Taipa, Macau; mthui@must.edu.mo
[2] Department of Physics and Astronomy, The University of Western Ontario, London, ON N6A 3K7, Canada
[3] Institute for Earth and Space Exploration, The University of Western Ontario, London, ON N6A 3K7, Canada
[4] Institute for Astronomy, University of Hawai'i, 2680 Woodlawn Drive, Honolulu, HI 96822, USA
Received 2021 October 29; revised 2021 November 6; accepted 2021 November 8; published 2021 November 23

Abstract

The Earth Trojans are coorbitals librating around the Lagrange points L_4 or L_5 of the Sun–Earth system. Although many numerical studies suggest that they can maintain their dynamical status and be stable on timescales up to a few tens of thousands of years or even longer, they remain an elusive population. Thus far only one transient member (2010 TK₇) has been discovered serendipitously. Here, we present a dynamical study of asteroid 2020 XL₅. With our meticulous follow-up astrometric observations of the object, we confirmed that it is a new Earth Trojan. However, its eccentric orbit brings it close encounters with Venus on a frequent basis. Based on our N-body integration, we found that the asteroid was captured into the current Earth Trojan status in the fifteenth century, and then it has a likelihood of 99.5% to leave the L_4 region within the next ∼10 kyr. Therefore, it is most likely that 2020 XL₅ is dynamically unstable over this timescale.

Unified Astronomy Thesaurus concepts: Asteroids (72); Near-Earth objects (1092); Trojan asteroids (1715)

1. Introduction

Trojans are small bodies in 1:1 mean-motion resonance (MMR) with a planet, librating around the Lagrange points L_4 or L_5 of the Sun–planet system. Numerous researchers (e.g., Rabe 1967; Mikkola & Innanen 1992; Tabachnik & Evans 2000; Brasser & Lehto 2002; Ćuk et al. 2012; Christou & Georgakarakos 2021; Marzari & Scholl 2013; Zhou et al. 2019, and many more) have performed theoretical and numerical studies on dynamical stability of Trojans and other types of coorbitals of solar system planets.

In the past century, over 10,000 Trojans have been recognized, the vast majority of which belong to Jupiter. In contrast, only one Earth Trojan (asteroid 2010 TK₇) has been identified, the discovery of which was in a serendipitous way by the Wide-field Infrared Survey Explorer mission in space (Connors et al. 2011). Ironically, all dedicated Earth Trojan surveys have found nothing (e.g., Whiteley & Tholen 1998; Markwardt et al. 2020; Lifset et al. 2021), owing to the fact that the observing circumstances of these objects are never ideal for ground-based telescopes, because they are always at small solar elongations. Moreover, such a survey will have to cover a huge sky area where Earth Trojans are potentially residing because of their proximity to Earth and libration around the Lagrange points (Wiegert et al. 2000).

Dynamical studies (e.g., Marzari & Scholl 2013; Zhou et al. 2019) indicate that low-inclination Earth Trojans have the potential to survive the age of the solar system, and therefore these long-term stable members could be primordial planetesimal remnants formed in situ near the Earth–Moon system in the protoplanetary disk. However, none of this subgroup of Earth Trojans has been discovered yet. In comparison, Mars has several Trojans that are dynamically stable over the age of the solar system (e.g., Scholl et al. 2005; de La Fuente Marcos & de La Fuente Marcos 2013). The only known Earth Trojan 2010 TK₇ is dynamically stable in the 1:1 MMR with Earth for

merely ≲25 Myr, and therefore it was most likely captured from elsewhere as a near-Earth asteroid (Dvorak et al. 2012).

Recently, asteroid 2020 XL₅ was discovered by the Panoramic Survey Telescope and Rapid Response System (Pan-STARRS 1) telescope at Haleakala Observatory, Hawai'i, on 2020 December 12,[5] and was suspected to be a potential candidate of the Earth Trojan population (de la Fuente Marcos & de la Fuente Marcos 2021). Thanks to our follow-up astrometric observations, we report our conclusive identification of asteroid 2020 XL₅ as the second transient Earth Trojan, confirming the study by de la Fuente Marcos & de la Fuente Marcos (2021) based upon a much shorter observing arc of the object. We describe our follow-up observations in Section 2 and present a dynamical analysis of the asteroid in Section 3.

2. Observation

We obtained follow-up observations of 2020 XL₅ using the University of Hawai'i (UH) 2.2 m telescope atop Maunakea, Hawai'i, on UT 2021 January 8, and September 12 and 13. In the first observing night, the observations were acquired through the Tektronix CCD in the on-chip 2×2 binning mode, rendering us an angular resolution of $0\rlap{.}''44$ pixel^{-1} with a field of view (FOV) of $7\rlap{.}'5 \times 7\rlap{.}'5$. In the remaining observing nights, we employed the STAcam CCD, which has been in use since 2021 April. To achieve critically sampling the typical seeing on Maunakea, the STAcam images were 5×5 binned, resulting in a pixel scale of $0\rlap{.}''41$ and an image dimension of 2112×2112 pixels. Individual images from 2021 January 8 have exposures of 60 and 90 s, while those from 2021 September have a common exposure of 8 minutes. In order to maximize collecting photons from the asteroid, we did not employ any filter, and the telescope was tracked nonsidereally at the apparent motion rate of the target. During our observations, the weather remained totally clear.

We performed astrometric measurements for our follow-up observations. Since our observations were tracked nonsidereally, all of the field stars in the same FOV alongside the target

---

[5] https://www.minorplanetcenter.net/mpec/K20/K20XH1.html

Table 1
Our Follow-up Astrometric Observations of 2020 XL$_5$

Observation Time (UTC)	R.A. (^{h} ^{m} ^{s}) α	Decl. ($^\circ$ $'$ $''$) δ	1σ Uncertainty ($''$)		O–C Residuals[a] ($''$)	
			E-W ($\Delta\alpha\cos\delta$)	Decl. ($\Delta\delta$)	E-W	Decl.
2021 Jan 08.661324	14 33 49.544	−19 59 19.23	0.075	0.075	+0.028	−0.013
2021 Jan 08.666390	14 33 51.824	−19 59 21.33	0.071	0.070	−0.020	+0.015
2021 Sep 12.610790	07 07 42.372	+09 42 55.34	0.066	0.066	−0.061	−0.036
2021 Sep 12.616674	07 07 43.246	+09 42 52.64	0.095	0.095	−0.039	+0.073
2021 Sep 12.622738	07 07 44.143	+09 42 49.72	0.066	0.066	−0.067	+0.049
2021 Sep 13.617119	07 10 13.089	+09 34 46.08	0.045	0.045	+0.018	−0.019
2021 Sep 13.623080	07 10 13.974	+09 34 43.20	0.054	0.054	+0.046	+0.002

Notes. The coordinates are referred to the Earth mean equator and equinox of J2000 system. Technically the uncertainty and residuals in the R.A. direction are essentially in the east–west (E-W) direction on the corresponding great circle in the celestial sphere.
[a] Observed minus calculated residuals in our best-fit orbital solution in Table 2.

were obviously trailed in the data, making conventional simple centroiding techniques inapplicable. To accommodate this, we treated each star trail as a trapezoid and Gaussian in the along-track and cross-track directions, respectively. In such a profile model, there are six free parameters in total to be fitted using the least-squares method, including the centroid's pixel coordinates, length, width, and position angle of the trail, and the peak pixel value of the trail profile model. The parameters were solved iteratively with determination of the sky background with adjacent pill-shaped annuli centered on the best-fit pixel coordinates of the centroids. With the obtained pixel coordinates, our code then used the least-squares method to find the astrometric plate constants with the Gaia DR2 catalog (Gaia Collaboration et al. 2018), whereby we could then convert the pixel coordinates of 2020 XL$_5$, whose image profile was simply treated as a bidimensional Gaussian, to the R.A. and decl. coordinates in the J2000 system. The astrometric measurement uncertainties were estimated via error propagation by assuming the Poisson statistics for the observing data. Our results are tabulated in Table 1. We estimated the seeing using the FWHM of the asteroid as well as the FWHM of star trails in the cross-track direction, finding that the values varied between ~0$''$6 and 1$''$0 from night to night.

3. Dynamics

In order to investigate the dynamical status of 2020 XL$_5$, we updated its orbit with our astrometry together with astrometric measurements by other observers, including the Catalina Sky Surveys, Pan-STARRS 1, and a few others. These observations were obtained through querying the Minor Planet Center (MPC) Database.[6] Since there is no available information regarding the astrometric measurement uncertainties from these observers, we had to adopt the weighting scheme described in detail by Vereš et al. (2017) for them. Moreover, the observations were also debiased in accordance with Farnocchia et al. (2015). We then refined the orbital elements of 2020 XL$_5$ using the orbit determination package EXORB8 written by A. Vitagliano, in which the planetary and lunar ephemerides DE431 (Folkner et al. 2014) are utilized and perturbations from the eight major planets, Pluto, the Moon, and the 16 most massive asteroids as well as post-Newtonian corrections are all incorporated.[7] We summarize our best-fit orbital elements for 2020 XL$_5$ as well as the associated

---

Table 2
Our Best-fit Orbital Solution for New Earth Trojan 2020 XL$_5$ (Heliocentric Ecliptic J2000.0)

Quantity		Value
Semimajor axis (au)	a	1.00076222(54)
Eccentricity	e	0.3871541(17)
Inclination ($^\circ$)	i	13.846827(10)
Longitude of ascending node ($^\circ$)	Ω	153.598852(87)
Argument of perihelion ($^\circ$)	ω	87.984486(98)
Mean Anomaly ($^\circ$)	M	262.41609(13)
Weighted rms residuals ($''$)		0.112
# of observations		27
Observed arc		2020 Nov 26-2021 Sep 13

Note. The orbital elements are referred to an osculation epoch of Barycentric Dynamical Time (TBD) 2020 November 26.5 = JD 2,459,180.0. The reported uncertainties (noted in the parentheses for concision) are all 1σ formal errors propagated from the astrometric measurement uncertainties.

1σ formal errors, which were calculated from the obtained covariance matrix propagated from the astrometric measurement uncertainties, in Table 2. In the solution, all of the observations were found to have astrometric residuals within the assigned or measured error bars, indicating that our adoption of the weighting scheme is reasonable. We show the astrometric residuals of our follow-up observations in the best-fit solution in Table 1.

We then created 1000 Monte Carlo (MC) orbital clones for 2020 XL$_5$ based on the obtained covariance matrix of the orbital elements according to the Cholesky decomposition method, which were subsequently integrated by SOLEX12, an N-body integration standalone package accompanied by EXORB8. To maintain consistency, the exact same force model was applied. We thereby obtained the geometric heliocentric state vectors of the nominal orbit, orbital clones, major planets, the Moon, Pluto, and the 16 most massive asteroids referenced to the J2000 ecliptic as functions of different epochs. Since here we only care about whether 2020 XL$_5$ is a new Earth Trojan or not, we first computed the heliocentric Cartesian coordinates of the target in a nonuniformly rotating frame in which the Earth–Moon system barycenter (EMB) always lies on the x-axis, and the z-axis is defined by the normal of the heliocentric orbital plane of the EMB:

$$\begin{pmatrix} x \\ y \\ z \end{pmatrix} = \begin{pmatrix} \boldsymbol{r} \cdot \hat{\boldsymbol{r}}_{\text{EMB}} \\ \boldsymbol{r} - (\boldsymbol{r} \cdot \hat{\boldsymbol{n}}_{\text{EMB}})\hat{\boldsymbol{n}}_{\text{EMB}} - (\boldsymbol{r} \cdot \hat{\boldsymbol{r}}_{\text{EMB}})\hat{\boldsymbol{r}}_{\text{EMB}} \\ (\boldsymbol{r} \cdot \hat{\boldsymbol{n}}_{\text{EMB}})\hat{\boldsymbol{n}}_{\text{EMB}} \end{pmatrix}. \quad (1)$$
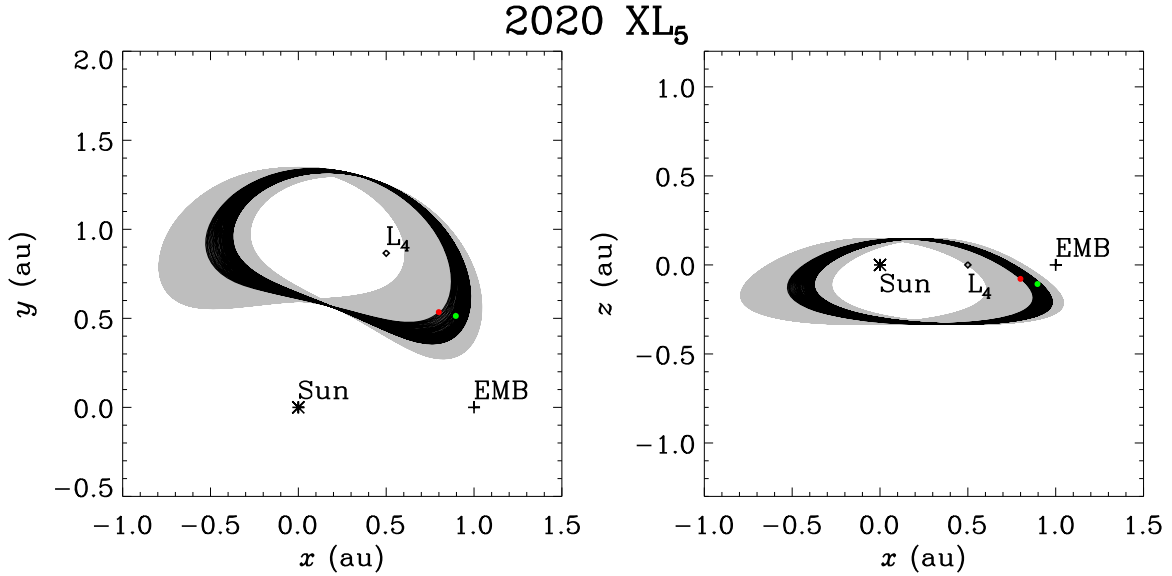
2020 XL$_5$

Figure 1. Trajectory of the new Earth Trojan 2020 XL$_5$ in the heliocentric frame corotating with the Earth–Moon barycenter (EMB, whose mean position is marked as the plus sign in the two panels) projected into the heliocentric orbital plane of the EMB (the *xy*-plane, left panel) and the *xz*-plane (right panel) from TDB 2021.0 to 2521.0. Also marked are the Sun (the asterisk) and the L_4 point. The red and green dots correspond to the starting and end points of the asteroid (moving clockwise in the *xy*-plane, and counterclockwise in the *xz*-plane). The section in black represents the trajectory of the asteroid in the first 50 yr of the timespan. Since the heliocentric orbit of the EMB is not circular but has a nonzero eccentricity, $e_{\mathrm{EMB}} \sim 0.01$, the epicycle of 2020 XL$_5$ shown here actually contains the contribution from the counterpart of the EMB, albeit much smaller.

Here, $\boldsymbol{r} = (X,\, Y,\, Z)^{\mathrm{T}}$ is the heliocentric position vector of 2020 XL$_5$, and $\hat{\boldsymbol{r}}_{\mathrm{EMB}}$ and $\hat{\boldsymbol{n}}_{\mathrm{EMB}}$ are respectively the unit radial vector and normal of the heliocentric orbital plane of the EMB, all expressed in the heliocentric J2000 ecliptic reference frame. In the rotating reference frame, L_4 and L_5 points are at $(1/2,\, \sqrt{3}/2, 0)^{\mathrm{T}}$ and $(1/2,\, -\sqrt{3}/2, 0)^{\mathrm{T}}$ au, respectively. We visually tracked the motion of the nominal and MC clones both backward and forward for 500 yr with a time step of 1 day in the *xy*-plane of the rotating reference frame, finding that all of them are moving around the L_4 point, which is indicative of 2020 XL$_5$ being a potential Earth Trojan (Figure 1).

However, such visualization alone does not provide us with any conclusive answer, because other coorbitals may behave similarly. So next, we converted the state vectors in the heliocentric J2000 ecliptic reference frame to heliocentric osculating orbital elements and computed the resonant argument in the 1:1 MMR configuration

$$
\begin{aligned}
\varphi &\equiv \lambda - \lambda_{\mathrm{EMB}} \\
&= (\varpi + M) - (\varpi_{\mathrm{EMB}} + M_{\mathrm{EMB}}),
\end{aligned} \tag{2}
$$

where λ, ϖ, and M are respectively the mean longitude, longitude of perihelion, and mean anomaly of the asteroid, and the quantities with the subscript "EMB" refer to those of the EMB system. For Trojans around the L_4 point their resonant arguments oscillate around $60°$, and those around the L_5 point will librate around $\varphi = -60°$, whereas other types of coorbitals have φ oscillating around $0°$ if they are quasi-satellites, or around $180°$ for horseshoe coorbitals. We show the evolution of the resonant argument of 10 of the clones alongside the nominal orbit from 5 kyr in the past to 10 kyr in the future in Figure 2, where we can see that, since the fifteenth century or thereabouts, 2020 XL$_5$ has been in the current dynamical status. Its resonant argument indeed oscillates close to but not about $\varphi = 60°$ in a libration period of $\sim$170 yr. We calculated

the libration period using the formula by Murray & Dermott (2000):

$$
T_{\mathrm{L}} = \frac{4\pi}{3} \sqrt{\frac{a_{\mathrm{EMB}}^3}{3G\mathcal{M}_{\mathrm{EMB}}}}. \tag{3}
$$

Here, $a_{\mathrm{EMB}} \approx 1$ au and $\mathcal{M}_{\mathrm{EMB}} \approx 6 \times 10^{24}$ are respectively the semimajor axis of the heliocentric orbit and total mass of the EMB system, and $G = 6.67 \times 10^{-11}$ m^3 kg^{-1} s^{-2} is the gravitational constant. Inserting numbers, we found $T_{\mathrm{L}} \approx 220$ yr, which is slightly longer than the observed period.

In order to understand the reason why the current libration of asteroid 2020 XL$_5$ is not about $\varphi = 60°$, we calculated its ponderomotive (effective) potential (Namouni et al. 1999)

$$
\Psi = \frac{1}{2\pi} \int_{-\pi}^{\pi} \left(\frac{1}{|\boldsymbol{r} - \boldsymbol{r}_{\mathrm{EMB}}|} - \boldsymbol{r} \cdot \boldsymbol{r}_{\mathrm{EMB}} \right) \mathrm{d}\lambda, \tag{4}
$$

where the position vectors are both expressed in au. Using the osculating orbital elements in Table 2, we plot the effective potential of the asteroid as the red curve in Figure 3, in comparison to that of the first Earth Trojan 2010 TK$_7$ in blue, whereupon we can observe that, while the minima of the latter are located basically around the Lagrange points L_4 and L_5, those of 2020 XL$_5$ are clearly shifted to larger resonant arguments in magnitude, due to the nontrivial orbital inclination and eccentricity. Therefore, we are now confident that 2020 XL$_5$ is currently in a tadpole orbit librating near the L_4 point, thus being the second known Earth Trojan after 2010 TK$_7$.

We proceed to investigate the orbital stability of 2020 XL$_5$. Unfortunately, chaos in its orbit prevents us from finding a conclusive answer pertinent to the exact history of 2020 XL$_5$ before its current dynamical status as an L_4 Earth Trojan. We calculated the Lyapunov timescale of the asteroid to be only a few hundred years by means of the tangent map method by Mikkola & Innanen (1999). Therefore, statistics from backward
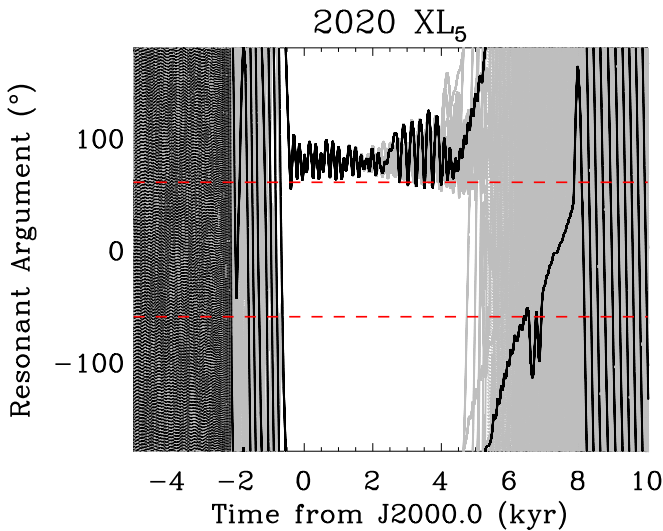
Figure 2. Temporal evolution of the resonant argument of asteroid 2020 XL$_5$ from BCE ~3000 to CE 12,000 with every 0.2 yr marked. The evolution of the nominal orbit is in black, whereas the MC clones (only 10 out of 1000 shown for clarity) are in gray. The upper and lower horizontal straight lines in red correspond to the L_4 and L_5 points of the Sun–EMB system. Our numerical simulation suggests that the asteroid has been librating around the L_4 point since the fifteenth century, thereby being an L_4 Earth Trojan, and will maintain the current status for another few millennia with a libration period of ~170 yr.
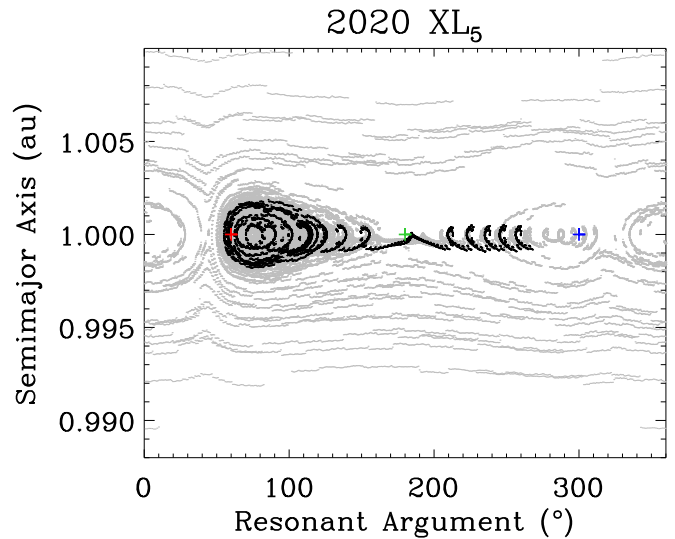
Figure 4. Phase portraits of 10 out of the 1000 MC orbital clones (gray) and the nominal orbit (black) in a timespan from CE ~5000 to 8000. The three crosses from left to right at the unity semimajor axis in au correspond to the three Lagrange points L_4, L_3, and L_5. Judging from the phase portraits, we can see that the while there are clones of 2020 XL$_5$ remaining as an L_4 Trojan, others may evolve into a transient L_5 Trojan, quasi-satellite, or may even leave the 1:1 MMR with the EMB. During this period, the nominal clone is gradually moving toward the L_5 point, as is also evidenced in Figure 2.
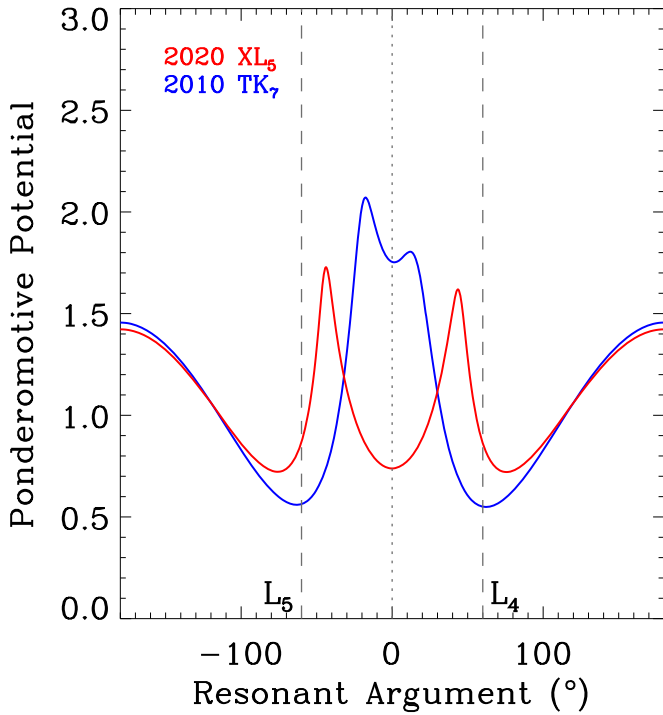
Figure 3. Comparison between the ponderomotive potentials of the two Earth Trojans 2020 XL$_5$ (red) and 2010 TK$_7$ (blue). Because of the nonzero inclination and eccentricity, minima of the effective potential are shifted away from $\pm 60°$ in the resonant argument, respectively, corresponding to the Lagrange points L_4 and L_5 (marked by two vertical dashed lines). The vertical dotted line marks the Sun–EMB direction.

integration of the clones for timespans much longer than the Lyapunov timescale are likely physically meaningless, because this may well cause a manifest increase in entropy of the system with time reversal, which clearly violates the second law of thermodynamics. Indeed, orbital evolution of the MC

clones and the nominal orbit in our backward integration prior to CE ~1000 is drastically different (for instance, in terms of the resonant argument, see Figure 2).

It is most likely that 2020 XL$_5$ will maintain its current Earth Trojan state for the next four millennia, whereafter its evolution becomes unclear again due to chaos in its orbit. Following Connors et al. (2011) and Dvorak et al. (2012), we visually examined the phase portraits of the nominal orbit and the MC orbital clones of 2020 XL$_5$ in the semimajor axis versus resonant argument space. Here, for clarity, only 10 of the MC clones alongside the nominal orbit are shown in Figure 4, where we can observe that while some of the clones remain in the current dynamical status as an L_4 Earth Trojan, others may become an L_5 Earth Trojan, quasi-satellite, or even leave the 1:1 MMR with the EMB.

In order to better characterize the timescale on which 2020 XL$_5$ remains as an Earth Trojan at the L_4 point, we tracked the nominal orbit and its 1000 MC orbital clones at each output time step (0.2 yr) in our numerical integration. In the forward simulation, whenever the resonant argument of a clone exceeds 180° for the very first time, we marked the corresponding epoch as the moment at which it has left the L_4 point. In the backward simulation, the latest epoch at which the clone has $\varphi \geqslant 180°$ was treated as the time when it started to be trapped in the L_4 region. The results are plotted in Figure 5. We found that 2020 XL$_5$ has been an L_4 Earth Trojan since CE 1444.7 ± 1.1, and ~99.5% of the clones (996 out of 1001 clones, including the nominal orbit) will leave the L_4 libration region within the next 10 kyr. We found the mean epoch when the clones exit the L_4 region to be 4.86 ± 0.51 kyr from J2000, where the uncertainty is the standard deviation. Therefore, it is highly likely that the 2020 XL$_5$ is dynamically unstable over the investigated period (~10 kyr), thus being the second transient Earth Trojan after 2010 TK$_7$. The latter became an L_4 Earth Trojan ~2 kyr ago and will maintain its current dynamical status for ~15 kyr before becoming a horseshoe
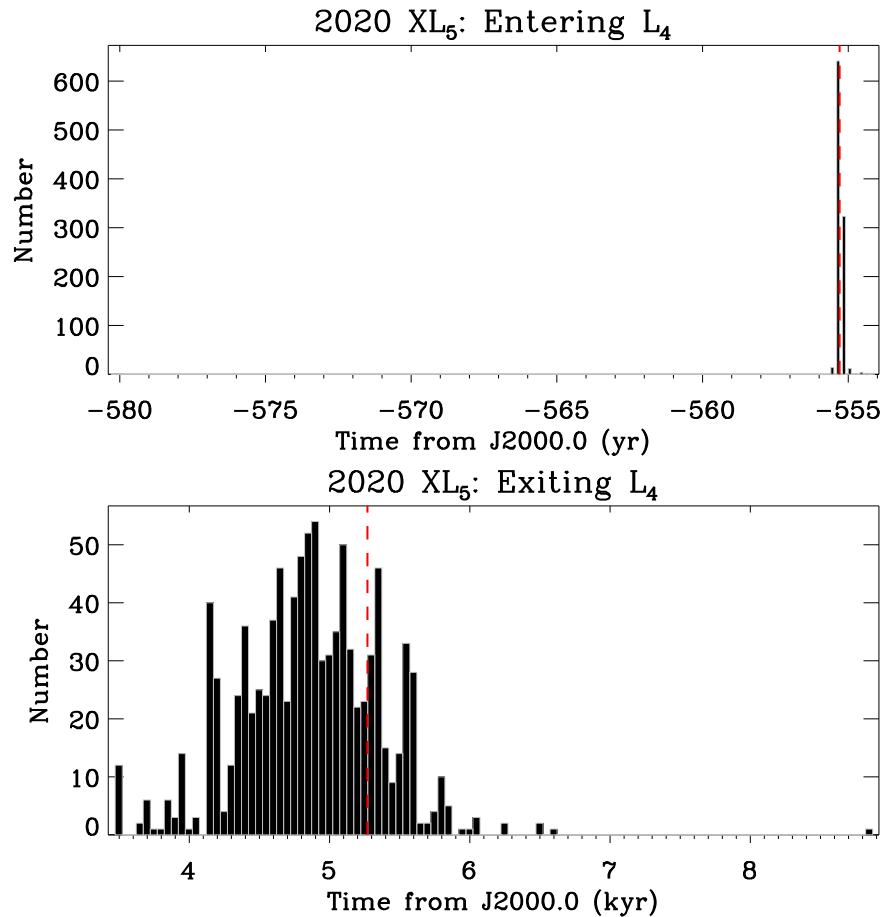
Figure 5. Statistics of the moments when the MC clones and the nominal orbit (red dashed line) enter (all of the clones) and leave (996 out of 1001 clones, or a fraction of 99.5%) the Lagrange L_4 points of the Sun–Earth system. Note that in the upper panel, there are two clones situated near the lower left corner, while the majority are distributed around CE ~1445. See Section 3 for details.

coorbital or jumping into the neighborhood of the L_5 point (Dvorak et al. 2012).

The short lifetime of 2020 XL$_5$ being on an Earth Trojan orbit is not unexpected, because its nontrivial eccentricity plus the relatively small orbital inclination makes it susceptible to the gravitational pulls of other terrestrial planets, in particular Venus, with which close encounters were found to occur on a common basis. Our finding agrees with the analysis by de la Fuente Marcos & de la Fuente Marcos (2021) based upon a much shorter observed arc of the object. With SOLEX12 we made use of the 1000 MC orbital clones in addition to the nominal orbit and searched for close encounters between the asteroid and various massive bodies in our force model described earlier in this section having mutual close approach distances $d_{min} \leqslant 0.1$ au from Barycentric Dynamical Time (TDB) 1900 January 1.0 to 2200 January 1.0. The results are summarized in Table 3, where we can see that in the examined three centuries, Venus is the only massive body that had and will continue having 10 close encounters with the Earth Trojan at mutual distances $\leqslant 0.1$ au in our search.

In the following, we use order-of-magnitude calculation to estimate the timescale on which 2020 XL$_5$ will leave the 1:1 MMR with Earth solely due to the perturbation from Venus. We only consider close encounters between the two bodies at $d_{min} \leqslant 0.1$ au. During one such close approach to Venus, the change in the orbital energy of 2020 XL$_5$ is due to the influence

of the Venusian gravitational potential

$$|\Delta E| = G\frac{\mathcal{M}_{\venus}\mathcal{M}}{d_{min}}, \tag{5}$$

where $\mathcal{M}_{\venus}$ and $\mathcal{M}$ are respectively the masses of Venus and 2020 XL$_5$, and $d_{min} \leqslant 0.1$ au is the close approach distance between the two bodies. In the two-body problem, the heliocentric orbital energy of 2020 XL$_5$ is given by

$$E = -G\frac{\mathcal{M}_{\odot}\mathcal{M}}{2a}. \tag{6}$$

Here, $\mathcal{M}_{\odot}$ is the mass of the Sun. Differentiating both sides, and equating the change in the orbital energy to the one by Equation (5), we find the change in the semimajor axis in the heliocentric orbit of 2020 XL$_5$ is

$$\Delta a = \frac{2a^2}{d_{min}}\left(\frac{\mathcal{M}_{\venus}}{\mathcal{M}_{\odot}}\right), \tag{7}$$

whereby we obtain that after a close encounter with Venus at $d_{min} \leqslant 0.1$ au, the Earth Trojan experiences a change of $\gtrsim 5 \times 10^{-5}$ au in semimajor axis in his heliocentric orbit. We approximate that 2020 XL$_5$ will stop being trapped in the 1:1 MMR with Earth once its semimajor axis differs from the one of Earth by over the Hill radius of the latter, which is $R_H \approx 0.01$ au. Despite that we did not check close encounters

Table 3
Close Encounters of 2020 XL$_5$ from TDB 1900 January 1 to 2200 January 1

Time (TDB)[a]	Body	Close Approach Distance (au)	Relative Speed (km s^{-1})
1979 Feb 01.8877 ± 0.0014	Venus	0.094141 ± 0.000013	11.23909 ± 0.00048
1987 Jan 28.6599 ± 0.0048	Venus	0.054339 ± 0.000065	12.7084 ± 0.0028
1995 Jan 27.4661 ± 0.0066	Venus	0.050302 ± 0.000090	12.8850 ± 0.0040
2003 Jan 29.0713 ± 0.0081	Venus	0.082103 ± 0.000092	11.6470 ± 0.0033
2054 Feb 12.7629 ± 0.0065	Venus	0.06122 ± 0.00013	16.7320 ± 0.0060
2062 Feb 12.5494 ± 0.0032	Venus	0.049010 ± 0.000058	16.1344 ± 0.0028
2070 Feb 10.5425 ± 0.0020	Venus	0.070863 ± 0.000041	17.1707 ± 0.0020
2179 Apr 04.878 ± 0.014	Venus	0.098895 ± 0.000022	13.891 ± 0.017
2190 Jan 30.540 ± 0.023	Venus	0.04856 ± 0.00040	16.001 ± 0.021
2198 Feb 01.512 ± 0.018	Venus	0.03767 ± 0.00019	13.676 ± 0.013

Notes. Our search for close encounters between asteroid 2020 XL$_5$ and the massive bodies in our force model was confined to a maximum close approach distance of 0.1 au. Under such configuration, Venus is the only planet that showed up in our search. The reported uncertainties are all standard deviations computed from the 1000 MC clones plus the nominal orbit.
[a] The corresponding uncertainties are in days.

between the asteroid and Venus outside the timespan from 1900 to 2200, we do not expect that the frequency of such encounters while 2020 XL$_5$ is still in the 1:1 MMR with Earth is significantly different. Accordingly, we estimate that a total number of ≲200 such close encounters with Venus will accumulatively destabilize the orbit of the Earth Trojan and gradually nudge it outside the 1:1 MMR with Earth. Given the expected occurrence frequency, the whole process will take merely ≲6 kyr, which agrees rather well with our N-body numerical simulation, demonstrating that Venus is the primary perturbation source that influence the coorbital status of 2020 XL$_5$ with Earth.

Note that in our analysis, we have completely omitted the Yarkovsky effect of the Earth Trojan due to anisotropic solar heating. However, we argue that our conclusions are not likely altered considerably even if there is such an effect. Following Farnocchia et al. (2013) and Hui & Jewitt (2017), we compute the expected drift rate in the semimajor axis of the heliocentric orbit of the asteroid by comparing to asteroid (101955) Bennu, in which way we will need a size estimate for 2020 XL$_5$. Using our photometry and that from the MPC, assuming a typical asteroidal phase slope of $G_\alpha = 0.15$ in the model by Bowell et al. (1989), we find the absolute magnitude of Earth Trojan to be $H = 20.4 \pm 0.5$ in the G band of the Gaia DR2 catalog. We further simply assume a typical geometric albedo of 0.1 for the asteroid, thus obtaining its nucleus radius to be $(1.6 \pm 0.4) \times 10^2$ m. Accordingly, we find the change rate in the semimajor axis of 2020 XL$_5$ is then $\sim 3 \times 10^{-3}$ au Myr^{-1}, which is by no means comparable to the corresponding change rate in the semimajor axis of the heliocentric orbit due to the perturbation by Venus. Therefore, we conclude that our omission of the Yarkovsky effect will not introduce any noticeable deviation from the reality.

4. Summary

The key conclusions of our study are listed as follows:

1. With our follow-up astrometric observations, we confirmed that 2020 XL$_5$ is a new Earth Trojan after 2010 TK$_7$.
2. 2020 XL$_5$ is only a transient Earth Trojan, as it has been librating around the L_4 point only since the fifteenth century, and its orbit is unstable on a ∼10 kyr timescale

primarily due to frequent close approaches to Venus at mutual distances of ≲0.1 au.
3. The minima of its current effective potential are clearly shifted away from 60° to a larger angle in the resonant argument because of its nontrivial orbital inclination and eccentricity.

Software: EXORB8, IDL, SOLEX12.

ORCID iDs

Man-To Hui (許文韜) ⓘ https://orcid.org/0000-0001-9067-7477
Paul A. Wiegert ⓘ https://orcid.org/0000-0002-1914-5352
David J. Tholen ⓘ https://orcid.org/0000-0003-0773-1888
Dora Föhring ⓘ https://orcid.org/0000-0001-9259-2688

References

Bowell, E., Hapke, B., Domingue, D., et al. 1989, in in Asteroids II, 524, ed. R. Binzel, T. Gehrels, & M. Matthews (Tucson, AZ: Univ. Arizona Press)
Brasser, R., & Lehto, H. J. 2002, MNRAS, 334, 241
Christou, A. A., & Georgakarakos, N. 2021, MNRAS, 507, 1640
Connors, M., Wiegert, P., & Veillet, C. 2011, Natur, 475, 481
Ćuk, M., Hamilton, D. P., Holman, M. J., et al. 2012, MNRAS, 426, 3051
de La Fuente Marcos, C., & de La Fuente Marcos, R. 2013, MNRAS, 432, L31
de la Fuente Marcos, C., & de la Fuente Marcos, R. 2021, RNAAS, 5, 29
Dvorak, R., Lhotka, C., & Zhou, L. 2012, A&A, 541, A127
Farnocchia, D., Chesley, S. R., Chamberlin, A. B., et al. 2015, Icar, 245, 94
Farnocchia, D., Chesley, S. R., Vokrouhlický, D., et al. 2013, Icar, 224, 1
Folkner, W. M., Williams, J. G., Boggs, D. H., Park, R. S., & Kuchynka, P. 2014, IPNPR, 42, 1
Gaia Collaboration, Brown, A. G. A., Vallenari, A., et al. 2018, A&A, 616, A1

Hui, M.-T., & Jewitt, D. 2017, AJ, 153, 80
Lifset, N., Golovich, N., Green, E., et al. 2021, AJ, 161, 282
Markwardt, L., Gerdes, D. W., Malhotra, R., et al. 2020, MNRAS, 492, 6105
Marzari, F., & Scholl, H. 2013, CeMDA, 117, 91
Mikkola, S., & Innanen, K. 1992, AJ, 104, 1641
Mikkola, S., & Innanen, K. 1999, CeMDA, 74, 59
Murray, C. D., & Dermott, S. F. 2000, Solar System Dynamics (Cambridge: Cambridge Univ. Press), 1999

Namouni, F., Christou, A. A., & Murray, C. D. 1999, PhRvL, 83, 2506
Rabe, E. 1967, AJ, 72, 10
Scholl, H., Marzari, F., & Tricarico, P. 2005, Icar, 175, 397
Tabachnik, S. A., & Evans, N. W. 2000, MNRAS, 319, 63
Vereš, P., Farnocchia, D., Chesley, S. R., et al. 2017, Icar, 296, 139
Whiteley, R. J., & Tholen, D. J. 1998, Icar, 136, 154
Wiegert, P., Innanen, K., & Mikkola, S. 2000, Icar, 145, 33
Zhou, L., Xu, Y.-B., Zhou, L.-Y., et al. 2019, A&A, 622, A97